ACS OMEGA

Article

http://pubs.acs.org/journal/acsodf

Radiopaque Hemocompatible Ruminant-Sourced Gut Material with Antimicrobial Physiognomies for Biomedical Applications in Diabetics

Nimmy K. Francis,[†] Harpreet S. Pawar,[†] Santanu Dhara,[‡] Anirban Mitra,[§] and Analava Mitra*[,†]

[†]Natural Products Research Laboratory and [‡]Biomaterials and Tissue Engineering Laboratory, School of Medical Science and Technology, Indian Institute of Technology Kharagpur, Kharagpur, West Bengal 721302, India

[§]Department of Computer Science & Engineering, Vignan Institute of Technology and Management, Berhampur, Odisha 761008, India

ABSTRACT: This study comprises the fabrication of a radiopaque gut material with its mechanical properties conforming to the US Pharmacopeia guidelines giving an antimicrobial advantage for suture application, especially in conditions such as diabetes mellitus, which has a high wound infection rate. Schiff base cross-linking iodination of the material is evinced by the spectroscopic studies, and antimicrobial properties owing to released iodine are evinced through in vitro studies. Modified gut sutures demonstrated favorable physicomechanical features such as appropriate tensile strength (440 ± 20 MPa) and knot strength (270 ± 20) alongside a mean radiopacity value of 139.0 ± 10 in comparison with that of the femoral shaft with 160 ± 10. The diabetic model showed absence of clinical signs of infection, supported by wound swab culture and the absence of necrosis in histology. Hemocompatibility studies evinced the absence of contact platelet activation and hemolysis alongside the customary coagulation response. These promising results highlight the stimulating potential of the process in the development of biomedical applications, necessitating persistent studies for its evidence-based applicability, particularly in diabetic patients.

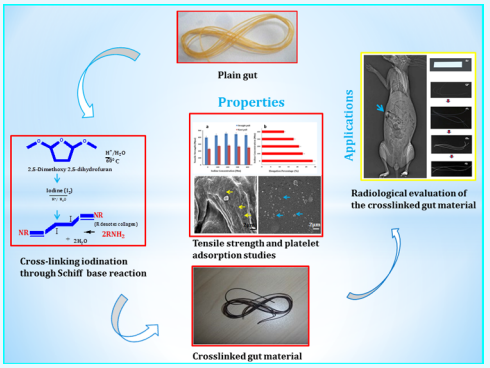

1. INTRODUCTION

Wound closure involves the approximation of edges of a wound or an incision using synthetic or natural materials to minimize infection and hemostasis and to restore normal function alongside good cosmetic outcome, depending on the location and type of the injury. Different suture materials differ in their physicomechanical and biological properties involving biocompatibility, degradation, knot security, tensile strength, wound security, and workability.[1] Diabetes mellitus (DM) remains a potential risk factor in the meta-analyses of studies for immediate postoperative wound infection, with an odds ratio of 1.53 in comparison to the normal.[2] Seventy-five percent of people with DM is expected to be from developing countries by 2025, with principal figures from India, China, and the United States, adding an economic burden of $490 billion for diabetic care by 2030.[3] Distorted innate cellular and humoral immune defense mechanisms with poor chemotaxis or phagocytosis by polymorphonuclear cells, genetic vulnerability, and local factors comprising poor blood flow and nerve damage are supposed to make diabetic candidates susceptible to wound site infections.[4]

Gut suture is a sterile absorbable surgical suture composed of purified connective tissues, principally collagen obtained from the bovine serosa layer or the ovine submucosal fibrous layer of intestines. They are available in plain or chromic variety and have been used as suture materials for many years in skin and soft tissue closure, oral, ophthalmic, orthopedic, gynecological, and gastrointestinal surgeries.[1,5−7]

Joseph Lister transformed surgery in the late 19th century by imparting the antimicrobial property to gut sutures by immersing them in a solution of carbolic acid in five parts olive oil and developing chromic gut that drastically reduced the incidence of infection, histrionically improvising patient health while enabling surgical approaches to advance rapidly.[8] Iodine is used as aqueous or alcoholic solutions and exerts a broad spectrum of antimicrobial activity, rapidly penetrating into microorganisms, attacking key groups of free-sulfur amino acids such as cysteine and methionine, nucleotides, and fatty acids, terminating in cell death. Iodine is also thought to confront the enveloped virus surface protein and also undermines membrane fatty acids by reacting with unsaturated carbon bonds.[9]

Radiopaque polymers can be used in dental prosthesis, vessel grafts, body fluids, and organ imaging, exploring its theranostic potential to be detected using noninvasive imaging techniques such as conventional X-rays and computed tomography (CT).[10−13] Ligand chelation using radiopacifying agents such as alkaline earth metal salts and polymerization of methyl

Received: November 8, 2016
Accepted: February 9, 2017
Published: March 2, 2017

DOI: 10.1021/acsomega.6b00373
ACS Omega 2017, 2, 755−764

methacrylate (MMA) with metal salts of vinyl monomers such as zinc or barium acrylates were used to prepare radiopaque polymers.[14−17] Embedding of electron-dense iodine-containing compounds such as triiodobenzoic acid and *N*-(2,6-diiodocarboxyphenyl)-3,4,5-triiodo benzamide into polymers such as cellulose, polymerization of aromatic iodine-containing vinyl monomers with monomers such as MMA and 2-hydroxyethyl methacrylate (HEMA), and cross-linking with iodine were carried out to deliver radiopacity.[18−22]

Introduction of hydrophobic nonbiodegradable polymers is known to cause anaphylactic reactions and neurological and cardiovascular symptoms.[23−25] Leaching of the contrast agents from a physically mixed heterogeneous composition such as $BaSO_4$ evokes undesirable biochemical responses such as the activation of osteoclasts.[26] Moreover aromatic benzene is reported to be genotoxic, causing DNA reactivity from free-radical-mediated oxidative damage, mutagenicity, and clastogenicity, instigating micronucleus, chromosomal aberrations from single- or double-strand breaks, aneuploidy, sister chromatid exchange, and aneugenesis.[27−29]

The present study aims at imparting radiopacity and antimicrobial features to the plain gut material using 2,5-dimethoxy-2,5-dihydrofuran (DMDF)−iodine cross-linking solution. Free amine groups of the collagen may be cross-linked by the iodine-linked bifunctional dialdehyde such as butenedial formed by the protolytic cleavage of DMDF via the Schiff base reaction.[22,30] The cross-linked material was then assessed for radiopacity, histocompatibility, degradation studies, antimicrobial features, and physicochemical and mechanical characteristics for suture application. Modified material may be helpful to curb the increasing incidence of postoperative infections, especially in diabetic patients with altered pathophysiologic orientation, with evidence-based support fit to the optimized quality yield to support the altered homeostasis.

2. MATERIALS AND METHODS

2.1. Materials. Chemicals of analytical grade including DMDF, iodine, silver nitrate ($AgNO_3$), ninhydrin reagent, collagenase IIa, and alloxan were procured from Sigma-Aldrich and used without further refinement. Ethicon plain gut 2′0 sutures and Accu-Chek glucometer with advantage II strips were also used.

2.2. Methods. *2.2.1. Suture Cross-Linking.* Gut sutures were cross-linked with a suitable DMDF cross-linking fraction ascertained using ninhydrin assay, using glycine after treatment with alcohol to remove the surface wax.[31] Air-dried samples were treated with different concentrations of DMDF solution at acidic pH and heated with 0.1% ninhydrin solution in 75° water bath for 20 min. Untreated sutures served as control, and a UV−visible spectrophotometer (Shimadzu UV-1601) was used to measure the absorbance standard. Different concentrations of iodine solutions (60, 80, 100, 200, 300, and 400) were prepared in 10% DMDF as per the ninhydrin assay result, in properly sealed glassware. Plain gut sutures were cross-linked with the prepared DMDF−iodine solution for 30 s, rinsed in distilled water to remove any unreacted iodine, and air-dried.[22,32]

2.2.2. Characterization of Fibers. 2.2.2.1. In Vitro and In Vivo Imaging. In vitro radiopacities of the DMDF−iodine cross-linked gut suture (CDI) and plain gut suture (CP) were tested against a lead sheet of 0.06 mm thickness as control by X-ray irradiation using a customary clinical X-ray instrument (Allenger's 325 X-ray system, 40 kW). Ethanol-sterilized CDI sutures of desired tensile strength properties for suture application and CP (control) were implanted in a rabbit animal model under aseptic . Rabbits were immobilized during scan by inoculating 0.5 mg/kg midazolam IM in the caudal thigh muscle and scanned using a Siemens somatom spirit dual-slice clinical CT scan.

2.2.2.2. Mechanical Testing and Knot Strength. A universal testing machine (Hounsfield, model H25KS, Redhill, England) was used to evaluate the tensile strength of gut sutures cross-linked with various strengths of DMDF−iodine. The straight-pull and knot-pull strengths of the gut suture with 0.3 mm diameter were tested at a speed of 55 mm/min and a gauge length of 3 cm as per the US Pharmacopeia (USP) guidelines for tensile-strength testing of surgical sutures.[33] The percentage elongation of the samples was also observed. Each experiment was performed in triplicate.

2.2.2.3. Energy Dispersive X-ray (EDX) Spectroscopy and Scanning Electron Microscopy (SEM). A scanning electron microscope (SUPRA-40, Carl Zeiss, Germany) attached with an energy dispersive X-ray spectrometer (Oxford Instruments Ltd., UK) was used to analyze the CDI and CP samples. Elemental assay of the sample was undertaken using EDX without gold coating. Air-dried samples were encrusted with a thin layer of gold using plasma sputter-coating before SEM observation. Iodine concentrations on the surface and at transverse cross sections were analyzed by taking an average of point analysis at various sites on different fibers.

2.2.2.4. X-ray Photoelectron Spectroscopy (XPS). Samples were chemically characterized using PHI Versa Probe II Scanning XPS Microprobe with monochromatic Al Kα radiation under ultrahigh vacuum. A 100 V to 5 kV differentially impelled argon ion gun was used for cleaning the specimen before measurement.

2.2.2.5. Fourier Transform Infrared (FTIR) Spectroscopy. Nexus-870 Perkin Elmer Spectrophotometer with a wavelength range of 400−3800 cm^{-1} was used to perform FTIR analysis of the CDI and CP samples after flattening them in a diamond compression cell. All measurements were performed under controlled humidity conditions in the absorbance mode at room temperature.[34]

2.2.2.6. Antimicrobial Testing. A bacterial suspension in a nutrient broth was used for optical density (OD) measurements for the antimicrobial activity of the iodinated collagen material sample. Luria broth (6 mL) with 50 μL of *Escherichia coli* (Gram-negative bacilli) and *Staphylococcus aureus* (Gram-positive, facultative anaerobe) inoculum, each with and without the CDI sample was kept on a shaking rotator at 37 °C. The OD was measured at different time points within 24 h of incubation at 600 nm using a spectrophotometer. Bacterial lawn cultures were also performed on Muller Hinton agar plates (Kirby−Bauer method) to test the antimicrobial effect of the CDI samples. *S. aureus* and *E. coli* suspensions were seeded on distinct sterile Muller Hinton agar Petri plates and incubated for 48 h at 37 °C. The samples were organized into a small clothlike pattern and placed on the *S. aureus* and *E. coli* lawn cultures, and the zone of inhibition was observed for each sample on the subsequent day.[35]

2.2.2.7. Cellular Viability Study. The cell viability and biocompatibility of the CDI sample was assayed using MTT [3-(4,5-dimethylthiazol-2-yl)-2,5-diphenyltetrazolium bromide]. Dulbecco's modified Eagle's medium (DMEM) supplemented with 10% fetal bovine serum, 100 U/mL penicillin, 100 μg/mL streptomycin, and 1% glutamine was used to culture the 3T3

DOI: 10.1021/acsomega.6b00373
ACS Omega 2017, 2, 755−764

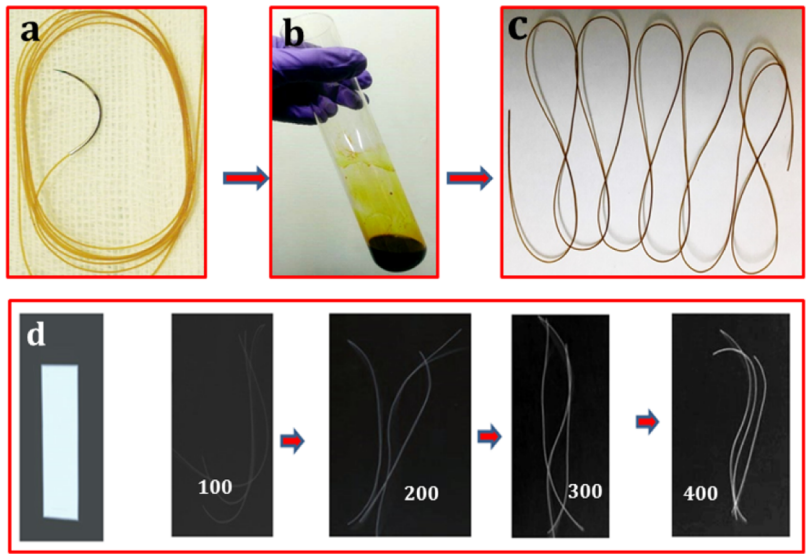

Figure 1. DMDF cross-linked gut suture preparation: (a) un-cross-linked gut; (b) cross-linking solution; (c) cross-linked gut suture; and (d) in vitro radiopacity of the lead sheet (control) and 100−400 mM iodine-treated sutures.

fibroblast cell line at 37 °C in a 5% CO_2 environment. The CDI sample was sterilized with 70% alcohol followed by rinsing with sterile phosphate-buffered saline (PBS) and incubated overnight in DMEM media for cell seeding. A medium without sample served as the control. The samples were seeded with 1 mL of resuspended cell culture having 1.1×10^5 cells/mL in a 9-well plate. MTT (20 μL, 5 mg/mL in PBS) was added to each well and incubated for 4 h on specific days. Dimethyl sulfoxide (100 μL) was added to each well to dissolve the dark blue formazan crystals formed from the reduction of MTT by the active cells, and the plate was kept on a shaker for 10 min. Absorbance was evaluated using a microplate reader (Bio-RAD 680, USA) with a reference filter at 620 nm.[35] SEM imaging was performed on day 3 for assessing the surface adhesion and cellular morphology of the CDI sample. The mean values were compared using one-way analysis of variance (ANOVA) followed by independent-samples *t*-test.

2.2.2.8. In Vitro Degradation. In vitro degradation was assessed by the change in the weight of the suture samples on incubation in 1 U/mL collagenase IIa in PBS as the test medium and plain PBS as the control medium at 37 °C. Vacuum-dried CDI and CP samples of 10 mg each were incubated with the test and control media, which were refreshed every alternate day. The samples were gathered carefully at definite time intervals over 3 days and vacuum-dried, following rinsing with PBS for weight measurement to calculate the percentage change in dry weight. SEM and EDX were performed to study the change in surface morphology and surface and core iodine concentration, respectively, on specified days during degradation studies. Mechanical strength assessment was performed for the CDI and CP samples using the straight-pull method at 55 mm/min as per the USP guidelines after 12 and 36 h. Each experiment was performed in triplicates, and the values were averaged.

2.2.2.9. Animal Model Preparation. Investigations on animals were carried out in adult male New Zealand white rabbits to evaluate in vivo degradation and histologic response, in agreement with the recommendations of the Institutional Animal Ethical Use Committee (SRGI/COP/SAEC/AM-IITYKGP/16/01). The animals were kept well-fed under a controlled environment with an alternate light/dark cycle. Midazolam (0.5 mg/kg) was injected intramuscularly in caudal thigh to attain sedation. Hair was removed from the back of the ear, and the area was cleansed with 70% alcohol. Alloxan (100 mg/kg) was prepared in 15 mL saline and administered through an ear vein, using a butterfly syringe by slow infusion. The treated rabbits were provided with a sugar solution for the next 2 d to avoid potential hypoglycemic shock. The blood glucose level was monitored daily using blood glucose test strips, and those with blood glucose levels >250 mg/dL (13.9 mmol/dL) were used in the study. Food and water intake were observed daily, and insulin treatment was entailed to control hyperglycemia as per the blood-glucose-level assessment.[36]

2.2.2.10. In Vivo Degradation and Histological Studies. After 7 days of alloxan treatment, the rabbits were sedated for 30 min using an intramuscular injection of midazolam (0.5 mg/kg) in the caudal thigh. The animals were kept in the prone position, and the implant location was shaved and cleansed with 70% alcohol. Local anesthesia was achieved using a hypodermal injection of 2% lignocaine, followed by the subcutaneous implantation of the CDI and CP samples under sterile conditions through an incision of width 1.5 cm. The wound was sutured and covered with gauze. The animals were sacrificed on day 6 and day 12 for mechanical strength testing of implants. The histocompatibility was assessed by taking a tissue sample along with the adjacent tissue. It was fixed in 4% formaldehyde in PBS followed by dehydrating with graded alcohol and paraffin wax embedding. Tissue sections were stained with hematoxylin and eosin (H&E) for cellular response and Van Gieson stain for collagen regeneration.[37]

2.2.2.11. In Vitro Hemocompatibilty. The slide method was used to calculate the clotting time by observing the fibrin strand formation time in the capillary blood collected aseptically. Whole blood without the sample served as control. Assays for prothrombin time (PT), thrombin time (TT), and activated partial thromboplastin time (aPTT or APTT) were performed to evaluate the thrombogenic behavior of the CDI sample by keeping it in whole blood collected in a citrate tube through central laboratory facilities. Percentage hemolysis was quantified from a colorimetric assay after incubating the CDI samples

DOI: 10.1021/acsomega.6b00373
ACS Omega 2017, 2, 755−764

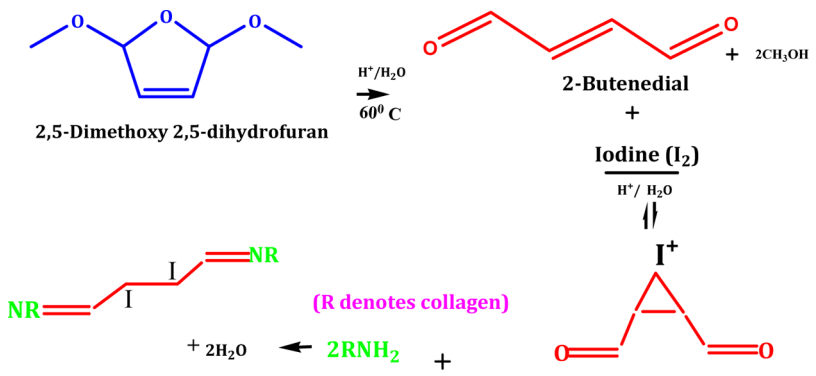

Figure 2. DMDF cross-linking of free amine groups of gut sutures butenedial intermediate.

with blood at 37 °C for 3 h, with gentle shaking every 30 min, followed by pelleting by centrifugation at the rate of 3000*g* for 15 min. Hemolysis in distilled water was taken as the control.[38] Whole blood without the sample was taken as reference for the study. The international normalized ratio (INR) was calculated for the sample. Platelet adsorption test was performed for the CDI sample by incubating the sample in platelet-rich plasma (PRP) diluted with PBS (1:1) for 15 min, followed by rinsing with PBS to eliminate the unadsorbed platelets. Samples were prepared for SEM (Zeiss Merlin Gemini II) after paraformaldehyde (3.7%) fixation. A glass coverslip was taken as control.

3. RESULTS AND DISCUSSION

Plain gut sutures appeared even-surfaced and dark in color after their treatment with a distinct concentration of DMDF−iodine solution, with intensification in color on increasing the iodine concentration (Figure 1). The optimal DMDF concentration for cross-linking was spectrophotometrically assessed using ninhydrin assay, which measures the free NH_2 functional group of the same. Un-cross-linked amines and alpha amino acids react with ninhydrin producing a colored compound named Ruheman's purple, whose spectrophotometric quantification gives an approximation of free amine groups.[39] The absorbance measured for the CP sample and samples cross-linked with 1 and 10% DMDF as per the glycine standard curve was 0.5 (0.3 mg/mL glycine), 0.2 (0.1 mg/mL glycine), and 0.09, respectively. The concentration against the absorbance value of 0.09 was not measurable on the standard curve, which echoes the near-complete amine group cross-linking; 10% DMDF concentration was used for further experimentation.

Iodinated gut suture may be the product of a staged chemical reaction involving amine moiety of the same with the difunctional butenedial formed from the protolytic cleavage of DMDF in acidic solution (Figure 2).[22,30] The electrophilic addition of molecular iodine on butenedial may result in the formation of 2,3-diiodo butenedial, involving an intermediate iodonium ion in acidic condition in the presence of an appropriate Lewis base such as alkene. Irving (1937) proposed a model of bridged halonium to elucidate the stereospecific formation of transhalogenation products, and iodine has proven to be a good bridging halide in comparison with other halides giving cardinal antiaddition products.[40]

Step-wise electrophilic addition of iodine, which acts as a Lewis acid to the π-bonding electrons of the bifunctional dialdehyde (butenedial) that acts as a Lewis base, may lead to the release of the iodide ion (I^-) and thence a bridged iodonium ion intermediate formation. Subsequent iodonium ring opening by nucleophilic gegenion (I^-) breaking the C−I bond may lead to the formation of vicinal di-iodide (2,3-diiodo butenedial). Endothermic iodination reaction follows multifaceted third-order reaction kinetics in polar solvents conditional to the structure of alkene and temperature. Several amino acids of various natural proteins such as glycine and tyrosine also develop adducts with molecular iodine as per previous studies.[40,41]

Nucleophilic attack by the nitrogen of the free amine group of lysine, hydroxylysine, or arginine within a collagen molecule or between adjacent collagens on the carbonyl moiety of 2,3-diiodo butenedial in a Schiff base reaction on the carbon of aldehyde may form C═N bond (imine bond) between collagen molecules. The temperature-controlled cross-linking property of DMDF in an acidic environment was exhibited in our previous work with surgical silk sutures, where the rate of cross-linking was enhanced with increasing concentration of DMDF.[22,42]

3.1. In Vitro and In Vivo Imaging. In vitro mean radiopacity values (MRVs) were calculated using the ImageJ software version 1.47 (NIH, USA) as the mean of five different points on a sample, and the results are shown in Table 1. The

Table 1. MRV for Gut Sutures Stained with Various Iodine Concentrations

test sample	iodine concn (mM)	MRV
control	0	0
CDI_{80}	80	70 ± 10
CDI_{100}	100	100 ± 9
CDI_{200}	200	115 ± 12
CDI_{300}	300	140 ± 10
CDI_{400}	400	160 ± 10
lead sheet	0	220 ± 4

MRV of CDI samples increased from 70 ± 10 to 160 ± 10 as the iodine concentration rose from 80 to 400 mM, as demonstrated in Figure 1d. A lead sheet of thickness 0.07 mm demonstrated an MRV of 210 ± 4, and the control sample (CP) was unremarkable. CDI gut sutures with 300 mM iodine was instituted to be effectual for the suture application as per the values of radio-opacity and tensile strength, consistent with the USP guidelines and thence used in further experiments in the study.[33] The in vivo MRV of CDI sutures on the first day on plain radiography was 140 ± 10 in comparison with that of the right femoral shaft with 160 ± 10 ($p < 0.05$). The MRV in conventional CT was 240 ± 8 in comparison to that of lumbar vertebrae 250 ± 1 ($p < 0.05$) (Figure 3).

DOI: 10.1021/acsomega.6b00373
ACS Omega 2017, 2, 755−764

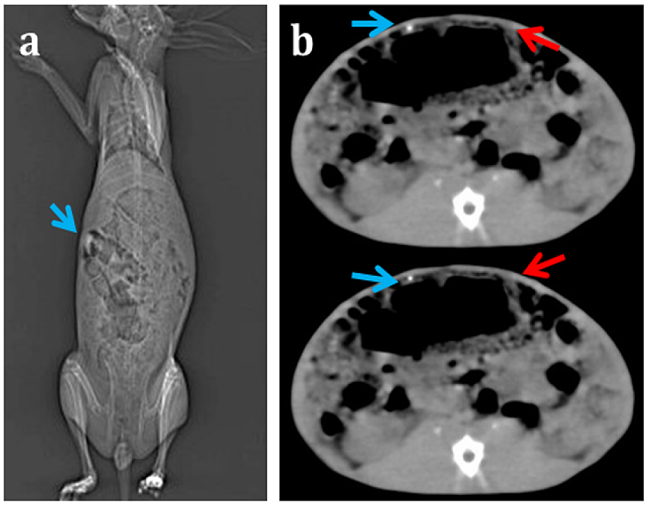

Figure 3. (a) In vivo plain radiography of CDI sutures in rabbit and (b) CT images of CDI implants (blue arrows) and plain gut sutures (red arrows) implanted at a symmetrically opposite location.

3.2. Mechanical Testing and Knot Strength. The key function of sutures is the approximation of a wide range of various tissue wounds, and thence the physiomechanical properties of the sutures are imperative for the selection and functioning of a suitable suture. The appropriate suture material should not rupture unpredictably along the usage, should elongate with edema at the site of injury, should be biocompatible, and should have appropriate knot security and a safe biodegradation profile.[8,43,44] The tensile strength and elongation percentage of the cross-linked gut sutures are shown in Figure 4. The tensile strength and the elongation percentage of the CP sample were 400 ± 10 MPa and 30 ± 3%, respectively. The tensile strength and the knot-pull strength of the CDI samples augmented from 430 ± 20 MPa (100 mM I_2) to 430 ± 20 (400 mM I_2) and 230 ± 10 MPa (100 mM I_2) to 250 ± 10 MPa (400 mM I_2), respectively, on cross-linking with DMDF−I_2. The elongation percentage decreased from 22.95 to 12.46% as the iodine concentration increased from 100 to 400 mM.

Increment in the tensile strength and reduction in the elongation percentage of fibers were noticed with increase in the iodine concentration in the cross-linking solution. This result can be explained by the breakage of intermolecular hydrogen bonding and polyiodide absorption in the amorphous protein regions changing the structural conformation. Molecular mobility is distorted by intramolecular or intermolecular cross-linking by altering the organization, increasing the rigidity of the fibers, decreasing the melt flow within the natural polymer, and hence declining the elongation percentage.[41] Excessive cross-linking caused the deterioration of the physiomechanical properties of the sutures.[45]

3.3. SEM and EDX. SEM demonstrates a smooth surface morphology of the CP sample when compared with CDI as shown in Figure 5a,b. DMDF−I_2 cross-linking may have instigated superficial roughing and specks seen on the fiber surface. According to the EDX results, the atomic weight percentage of iodine on the surface and the core of the CDI sample is 30 and 8, respectively, pertaining to carbon and oxygen (Figure 5d), and the CP sample is devoid of iodine. The presence of iodine in the crux attributes to in situ cross-linking reaction from the surface to the core.

3.4. XPS. Collagen is a protein with regular repetition of amino acids (glycine, proline, and hydroxyproline) and high glycine content, stabilizing the left-hand helix by expediting hydrogen bonding and intermolecular cross-linking with a relatively high carbon content on the surface as evidenced by dichroic studies.[46] The spectra of the CDI sample exhibit peaks of carbon, nitrogen, and oxygen levels at 285.56, 398.4, and 531.2 eV, respectively, in consonance with prior studies. The 3D XPS spectra of the CDI_{300} sample demonstrate a peak split which is in agreement with the 3d orbital split of iodine to $3d_{3/2}$ and $3d_{5/2}$, with energy levels around 619.3 and 631.8 eV, respectively (Figure 6a).[47] The presence of the covalently bound iodine and the absence of ionic iodine confirm the results of previous studies of C−I covalent bond, which is manifested by these binding energy levels.[48]

3.5. FTIR Analysis. The polypeptide chain configurations of the plain gut and the cross-linked one are exemplified by the characteristic absorption band study corresponding to the molecular conformation as per the FTIR spectrum (Figure 6b). The results indicate that the cross-linked suture materials maintained the triple helical arrangement of the collagen. The CP sample demonstrated bands at 1658, 1550, and 1244 cm^{-1},

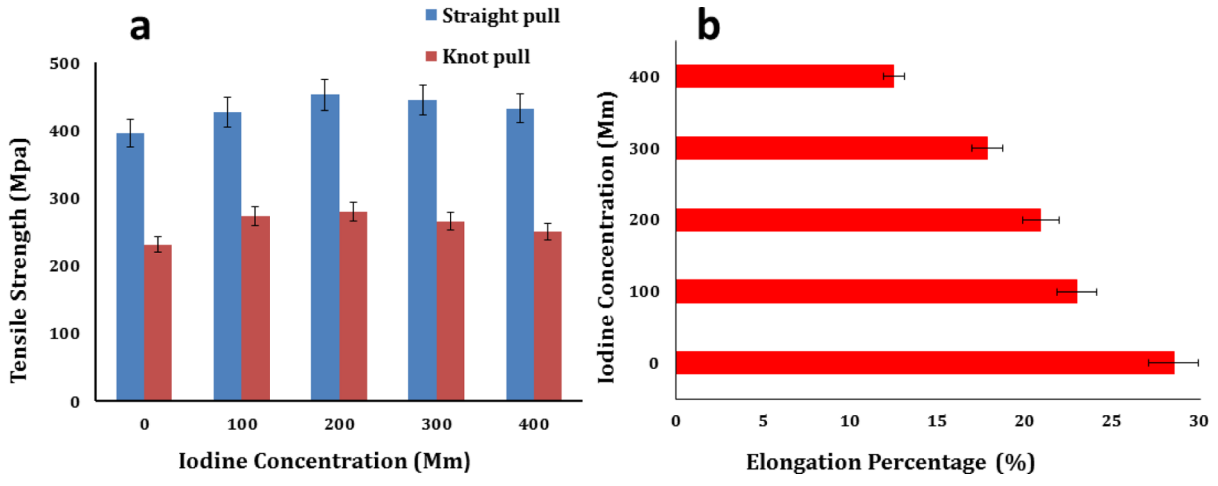

Figure 4. (a) Straight-pull and knot-pull tensile strength of the CP sample shown for zero iodine concentration and of CDI samples for increasing iodine concentration, and (b) change in the elongation percentage of cross-linked gut sutures.

DOI: 10.1021/acsomega.6b00373
ACS Omega 2017, 2, 755−764

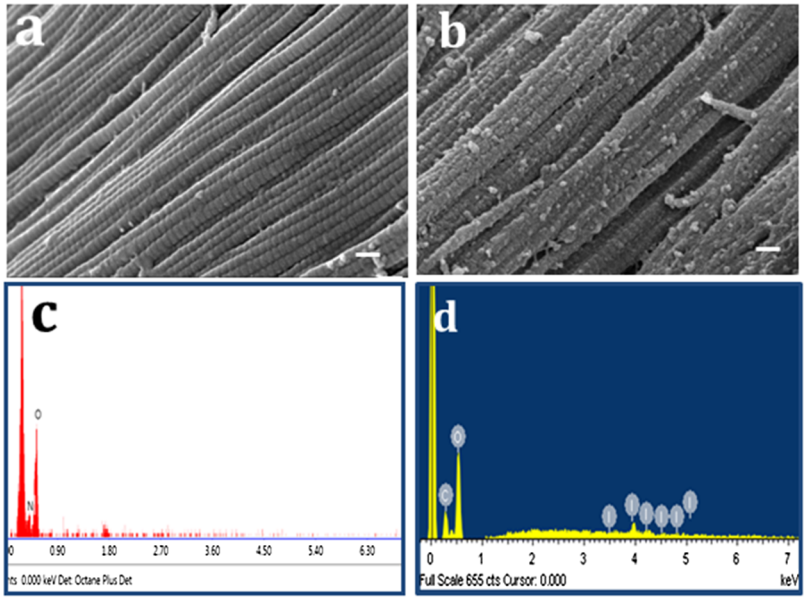

Figure 5. Surface morphology of (a) CP sample and (b) CDI sample using SEM (scale bar = 10 μm), (c) EDX analysis of the CP sample, and (d) EDX analysis of the CDI sample.

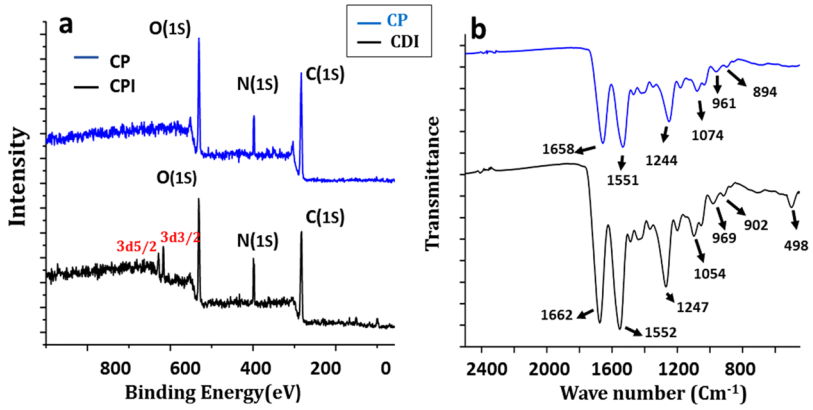

Figure 6. Chemical characterization of CP and CDI samples using (a) XPS and (b) FTIR spectroscopy.

characteristic of the amide I, II, and III bands, respectively. Amide I bands (1658 cm^{-1}) result from C═O stretching vibrations, amide II bands (1550 cm^{-1}) arise from the N−H bending vibrations coupled to C−N stretching vibrations, and amide III bands (1244 cm^{-1}) correspond to the combination peaks between N−H deformation and C−N stretching vibrations.[49] The absorption bands of amide I, amide II, and amide III shifted to 1662, 1552, and 1247 cm^{-1}, respectively, on CDI cross-linking, which is ascribed to the change in the molecular structure. Additionally, a shift to higher frequencies in the amide bands designating the cross-linking may be the result of the coordinate or H-bonding interactions of the amide nitrogen.[34,49,50] The distinguishing absorption bands of newly formed C═N and C−N bonds owing to cross-linking with DMDF are overlapped by those of amide I, amide II, and amide III. C−H bending vibrations of the methyne group (1000−650 cm^{-1}) stemmed from the absorption bands at 894 and 961 cm^{-1} in the CP sample and 902 and 969 cm^{-1} in the CDI sample.[22,49] Intra- and inter-molecular cross-linking of the aldehyde group of butenedial with the free amine groups of the collagen via the Schiff base reaction might have resulted in the new peaks. An additional peak of alkyl halide stretching (C−I) is seen at 498 cm^{-1} in the CDI sample.[51]

3.6. Antimicrobial Studies. The antimicrobial property of the iodinated collagen-based samples is accredited with the presence of iodine, and OD of the bacterial cultures augmented slowly up to 4 h followed by the growth of OD only in the control.[9,52] The OD values of *E. coli* cultures with the CDI sample were less than that of *S. aureus*. The OD values calculated for the CDI sample in *S. aureus* at 24 h (1.2 ± 0.02) were significantly lower than the control (1.9 ± 0.01) (p < 0.01). Similarly, the OD values for the CDI sample for the *E. coli* culture (1.1 ± 0.01) were substantially lower (p < 0.01) than the control (2.1 ± 0.01) at 24 h (Figure 7e). An irregular zone of inhibition was seen around the sample on the Petri plates after 24 h of incubation, as shown in Figure 7a,b. Iodine preparations, which have a vital role in the prevention of surgical site infections, are thought to provide the antimicrobial property mainly by rapidly penetrating the cell wall, unlike antibiotics that use definite molecular pathways, making them less susceptible to resistance.[9,53]

3.7. Cell Viability. The cytotoxicity of the CDI sample was assessed using MTT assay, which involves the quantitative

DOI: 10.1021/acsomega.6b00373
ACS Omega 2017, 2, 755−764

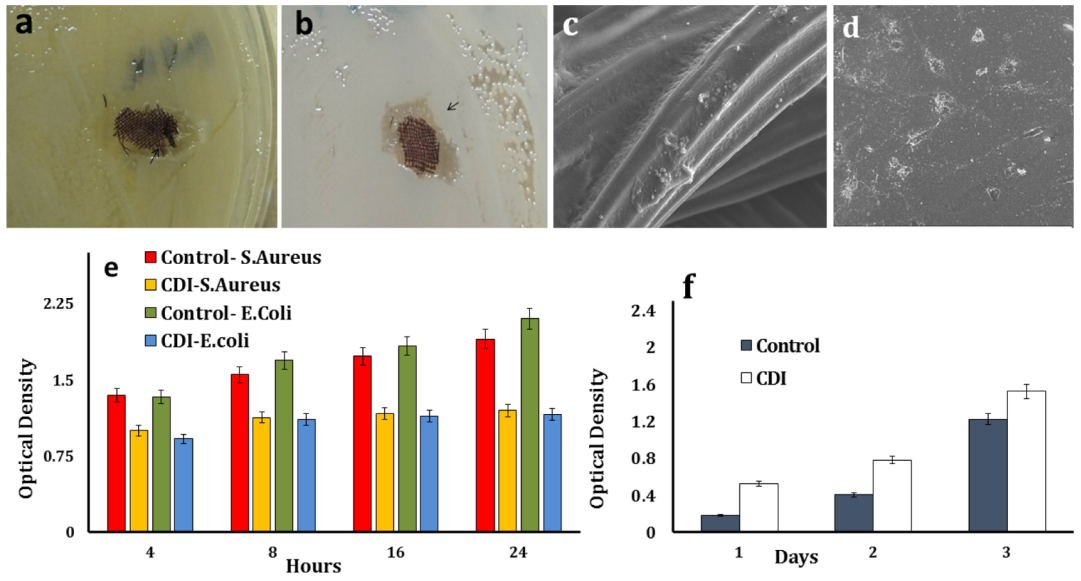

Figure 7. (a,b) Asymmetrical zone of inhibition (black arrow) seen in *E. coli* and *S. aureus* Petri plates. SEM images of 3T3 fibroblast cells growing on (c) CDI samples (scale bar = 40 μm) and (d) control (scale bar = 10 μm). (e) Optical densities of *S. aureus* and *E. coli* cultures with the iodinated collagen-based samples over 24 h of incubation and (f) optical densities of 3T3 fibroblast cells on the CDI sample compared with the CP sample on MTT assay.

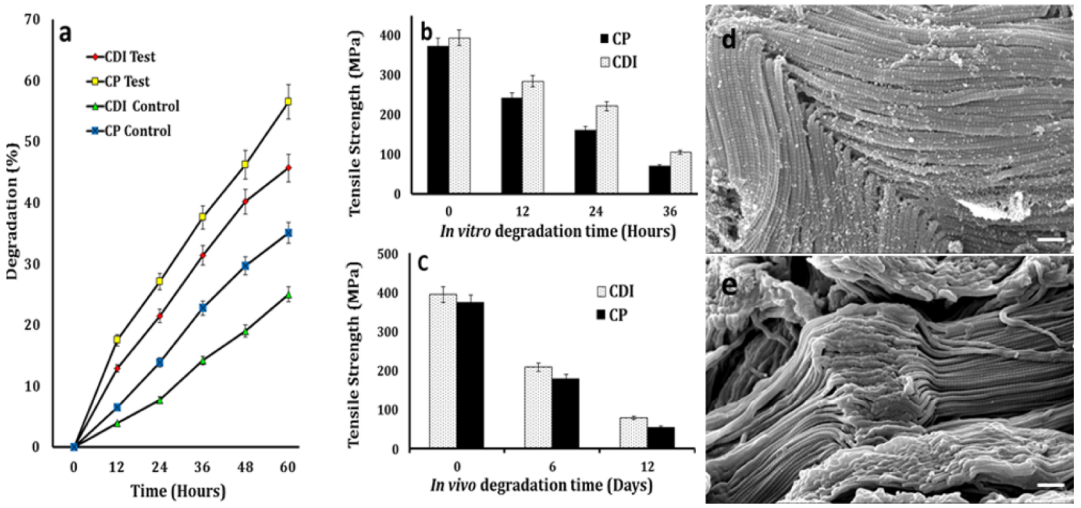

Figure 8. (a) Percentage of weight loss for CDI and CP samples in the collagenase IIa enzyme over 60 h. The control represents the samples in PBS; (b,c) in vitro and in vivo tensile strength reduction for the CDI and CP suture samples over 12 days; and (d,e) SEM images depicting the degradation of the CDI and CP samples in the collagenase IIa enzyme (scale bar = 1 μm).

estimation of living cells from the formation of dark blue formazan crystals due to mitochondrial enzyme activity.[54] Absorbance values were measured on the first, third, and fifth day of the assay (Figure 7f). Absorbance was pre-eminent for the CDI samples when equaled to that of the control, indicating the increased proliferation of the 3T3 fibroblast cell line on the former. The OD value for CDI samples was measured to be 1.5 ± 0.06, which contrasted with the control value of 1.2 ± 0.02 by the fifth day. The relative growth rate of cells on the CDI sample pertaining to the control was estimated to be (OD of test − OD of control)/(OD of test).[22] A high relative growth of 65% was observed on the CDI sample, which shrank progressively to 22% by the fifth day, which could be due to the comparatively early confluence of cells. The SEM images illustrate the CDI sample with a fibroblast cell attachment on the surface alongside interconnections and multipolar polygonal morphology, which is in compliance with the noncytotoxic behavior of the same.[50] The binding of iodine to an additional molecule makes it safe for clinical applications, aiding in the sustained release of iodine from the reservoir, as an alternative to high concentrations discharged in a single application[52] (Figure 7c,d).

3.8. In Vitro Degradation. Several proteases associated with inflammation comprising the endopeptidase cathepsin B and collagenase may be present at the wound site, catalyzing the hydrolysis of polypeptides. In the present investigation, in vitro degradation studies were undertaken using the collagenase IIa enzyme, which cleaves the bond between any neutral amino acid and glycine in a peptide sequence, degrading the triple-helical native collagen.[55] Dry weight measurement of samples was taken every 12 h, which gave the percentage weight loss following incubation at 37 °C. The CDI and CP samples

DOI: 10.1021/acsomega.6b00373
ACS Omega 2017, 2, 755−764

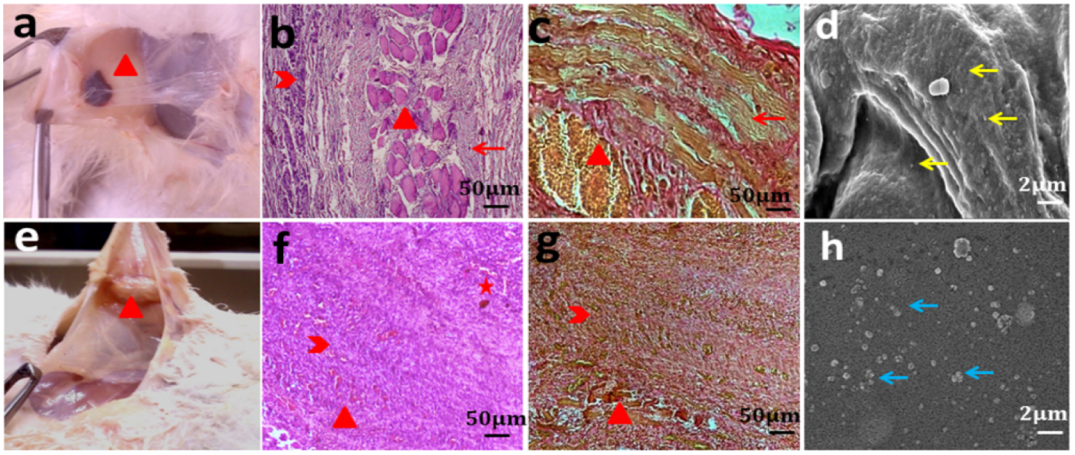

Figure 9. (a,e) CDI and CP sample retrieval, respectively; (b,f) H&E staining of the CDI and CP samples, respectively, at day 12; (c,g) VG staining of CDI and CP samples, respectively, at day 12; (d) yellow arrow indicating disk-shaped nonactivated platelets on CDI samples; and (e−h) blue arrow indicatingthe platelet clumps on coverslips (control) (red star, arrow head, cross, and arrow indicate neovascularization, mononuclear cell penetration, sample remnants, and fibrous tissue, respectively).

showed a weight loss of 46 ± 1 and 57 ± 0.9%, respectively, ($p < 0.01$) at the end of 60 h and a reduction in tensile strength to 27 and 19%, respectively, over 36 h (Figure 8a,b).

A small defect has an enormous effect on the strength of the fiber without having much influence on the fiber weight, and hence, tensile strength assessment appears to be more sensitive than other parameters in the evaluation of degradation.[56] The molecular weight of collagenase is 109 000, and the water content of the plain gut ranged from 45 to 60 wt %. The enzymatic hydrolysis of the suture is proposed to occur from its surface to the core despite the water present inside of the fiber, because of the large size of the enzyme molecule preventing its diffusion into the fiber and the poor water content of the swollen fiber. The reduction in mechanical strength reported in the degradation studies can be explained by the progression of defects at random sites of enzymatic cleavage along the fiber.[55] The CDI fibers in the degradation study appeared to be swollen and exhibited a coarse surface architecture with gradual emergence of fissures, specks, and accretions, which is attributed to the gradual surface proteolysis of the X−Gly peptide bonds by the enzyme collagenase.[57] The local defects thus created also diminish the mechanical property of the material.

3.9. In Vivo Degradation and Histological Studies. The rabbits with implanted CDI samples were healthy with no evident symptoms of acute inflammation such as rubor, calor, and tumor on clinical examination. The CDI and CP samples exhibited attrition of tensile strength to 20 and 16%, respectively, over 12 days (Figure 8c). Wound swab cultures were negative for pathognomonic organisms. Tensile strength degradation was found to be low ($p < 0.05$) for the CDI samples compared with CP in in vitro and in vivo studies over 12 d. CP sutures preserved substantial tensile strength for approximately 4 to 5 days.[1,43,44] In vivo and in vitro studies show considerable preservation of tensile strength until 12 days unlike plain gut sutures, which makes them befitting for mucosal applications that requires extended duration of wound security, abolishing the need for suture removal. It also results in the greatest amount of tissue reaction of all absorbable sutures. Tissue samples manifested neovascularization and histological response on day 12; the sections revealed suture remnants surrounded by fibrous tissue and multinucleate giant cells with macrophages indicative of foreign-body-type tissue reaction in the case of CDI samples.[42] No evidence of tissue edema and necrosis was observed. The CP samples were almost completely absorbed, leaving a few remnants and structured fibrous tissue replacing the damaged connective tissue alongside angiogenesis, indicating tissue healing. Minimal mononuclear cell infiltration was seen around the sample (Figure 9b,f). This was supported by VG staining, which showed more extensive and organized collagenous fibrosis (reddish brown color) for the pristine gut samples than the processed ones (Figure 9c,g). The results were in congruent with the histocompatible nature of the sample.[42]

3.10. In Vitro Hemocompatibility. Hemocompatibility assessment was performed to know the influence of the processed material on the coagulation cascade involving intrinsic, extrinsic, and common pathways for vascular application.[38] The PTs for citrated blood with and without the CDI sample were found to be 12.1 and 12.8 s, respectively, with the laboratory reference of 12.5 s. The INR was found to be 0.97 for the CDI sample. The aPTT and TT with and without the CDI sample were found to be 37.3 s and 36.5 s, and 12.9 s and 12.3 s, respectively, within the normal range. Normal PT and INR values of the blood specimens with CDI sample preclude any clotting factor inhibitory action and support favorable the clotting profile through the extrinsic or tissue factor pathway. A high INR indicates a higher risk of bleeding, whereas a low INR suggests a greater risk of developing a clot.[38,58] The aPTT quantifies the pace at which blood clots through two sequential series of biochemical reactions known as the intrinsic or contact activation pathway and the common coagulation pathway. The thrombin clotting time, also known as TT, quantifies the time taken for the clot formation in the blood sample containing the anticoagulant, after an excess addition of thrombin. The normal values of aPTT and TT exclude any atypical impact on the same.[38] The whole blood displayed fibrin strand formation on the glass slide (clotting time using the slide method) in 320 s in comparison to 340 s in the case of the CDI sample. The results are suggestive of the integrity of the intrinsic coagulative pathway on contact with the nonendothelial suture surface.[59,60] Thrombus formation initiates platelet adsorption on the material surface and its activation. The membrane damaging

DOI: 10.1021/acsomega.6b00373
ACS Omega 2017, 2, 755−764

potential of the CDI sample surface was evaluated through the colorimetric assay for hemolysis, which demonstrated a meager value of 2.1 ± 1% in comparison with distilled water (control). Nonactivated disc-shaped platelets were discretely distributed on the CDI sample surface in comparison with the platelet aggregate, suggestive of platelet activation observed on the control (glass cover slip), as shown in Figure 9.[60]

4. CONCLUSIONS

The plain gut-based absorbable suture is used in general soft tissue approximation and ligation in general closure, oral, ophthalmic, orthopedic, obstetric, and gastrointestinal surgeries, owing to its physicochemical and biological properties, depending on the patient condition, surgical experience, surgical technique, and wound size.[1,5−7] Diabetic patients,having impaired immune function and the inflammatory response are highly susceptible to infections in the immediate postoperative period. In the present study, DMDF−I_2 cross-linking method was performed to provide significant radiopacity to the plain gut sutures with added antimicrobial and hemocompatibility features, maintaining the inherent mechanical strength for envisioned surgical utilization, particularly in diabetic patients. The results demonstrate good biocompatibility supported by initial in vitro and in vivo histocompatibility studies in a diabetic rabbit model alongside admirable mechanical and handling properties of the resultant product in accordance with the USP recommendation. Radiopacity and tensile strength enhanced with increase in the iodine concentration in the DMDF−I_2 solution. The minimum strength required for clinical application as per the USP guidelines is 14.1 MPa. CDI (300 mM I_2) sutures (2′0) with 444.84 ± 23.3 MPa straight-pull tensile strength, 265.66 ± 16.8 MPa knot-pull strength, and an MRV of 139.0 ± 12.5 in comparison with the right femoral shaft having a value of 161.4 ± 11.3 were found to be most suitable for suture application. Preliminary hemocompatibility studies precluded thrombogenic and hemolytic features of the cross-linked gut material, evidencing normal coagulation cascade, which is vital for vascular applications. The material is easily processed via an economical procedure and has good visibility owing to the dark color attained following iodination, which precluded the need for additional dyes, and antimicrobial property owing to linked iodine release.

The results emphasize the stimulating potentials of the study in developing absorbable radiopaque, antimicrobial, hemocompatible, medical-grade polymers for biomedical applications such as surgical hernia mesh implants, embolic agents, sieves, and stents (vascular, urethral, or biliary), especially in immunocompromised conditions such as DM, simultaneously opening a theranostic realm in postoperative noninvasive follow-up.

AUTHOR INFORMATION

Corresponding Author

*E-mail: analavamitra@gmail.com, amitra@adm.iitkgp.ernet.in. http://iitkgp.ac.in/. http://vitam.edu.in/vitam/.

ORCID

Harpreet S. Pawar: 0000-0003-2926-4504

Analava Mitra: 0000-0003-2597-0794

Notes

The authors declare no competing financial interest.

ACKNOWLEDGMENTS

Authors would like to acknowledge Dr. Selva and Nantu Dogra for professional help and IIT Kharagpur for infrastructural facility.

REFERENCES

(1) Swanson, N. A.; Tromovitch, T. A. Suture materials, 1980s: Properties, uses, and abuses. *Int. J. Dermatol.* **1982**, *21*, 373−378.

(2) Martin, E. T.; Kaye, K. S.; Knott, C.; Nguyen, H.; Santarossa, M.; Evans, R.; Bertran, E.; Jaber, L. Diabetes and Risk of Surgical Site Infection: A Systematic Review and Meta-analysis. *Infect. Contr. Hosp. Epidemiol.* **2016**, *37*, 88−99.

(3) Francis, N. K.; Pawar, H. S.; Mitra, A.; Mitra, A. Rising Trend of Diabetes Mellitus amongst the Undernourished: State-of-the-Art Review. *Diabetes Metab. Syndr.: Clin. Res. Rev.* **2016**, DOI: 10.1016/j.dsx.2016.12.027.

(4) Geerlings, S. E.; Hoepelman, A. I. M. Immune dysfunction in patients with diabetes mellitus (DM). *FEMS Immunol. Med. Microbiol.* **1999**, *26*, 259−265.

(5) Harrisons, N. W. *Surgery of Female Incontinence*, 2nd ed.; Springer-Verlag: London, 1986.

(6) Roenigk's, P. W. R. *Dermatologic Surgery: Principles and Practice*, 2nd ed.; Marcel Dekker: New york, 1996.

(7) Rothrock, J. C. *Alexander's Care of the Patient in Surgery*, 15th ed.; Elsevier Mosby: Missouri, 2014.

(8) Muffly, T. M.; Tizzano, A. P.; Walters, M. D. The history and evolution of sutures in pelvic surgery. *J. R. Soc. Med.* **2011**, *104*, 107−112.

(9) McDonnell, G.; Russell, A. D. Antiseptics and Disinfectants: Activity, Action, and Resistance. *Clinical Microbiology Reviews* **1999**, *12*, 147−179.

(10) Guglielmi, G.; Benati, A.; Perini, S. Endovascular embolization with radiopaque silk threads: A feasibility study in Swine. *Intervent. Neuroradiol.* **2006**, *12*, 109−112.

(11) Bove, A. A.; Lazarow, N. H. Imaging system and method using radiopaque microspheres for evaluation of organ tissue perfusion. Google Patents, **1987**.

(12) Dawlee, S.; Jayakrishnan, A.; Jayabalan, M. Studies on novel radiopaque methyl methacrylate: Glycidyl methacrylate based polymer for biomedical applications. *J. Mater. Sci.: Mater. Med.* **2009**, *20*, S243−S250.

(13) Aviv, H.; Bartling, S.; Kieslling, F.; Margel, S. Radiopaque iodinated copolymeric nanoparticles for X-ray imaging applications. *Biomaterials* **2009**, *30*, 5610−5616.

(14) Thanoo, B. C.; Jayakrishnan, A. Barium sulphate-loaded p(HEMA) microspheres as artificial emboli: Preparation and properties. *Biomaterials* **1990**, *11*, 477−481.

(15) Thanoo, B. C.; Sunny, M. C.; Jayakrisnnan, A. Tantalum-loaded polyurethane microspheres for particulate embolization: Preparation and properties. *Biomaterials* **1991**, *12*, 525−528.

(16) Horák, D.; Metalová, M.; Švec, F.; Drobnik, J.; Kálal, J.; Borovička, M.; Adamyan, A. A.; Voronkova, O. S.; Gumargalieva, K. Z. Hydrogels in endovascular embolization. III. Radiopaque spherical particles, their preparation and properties. *Biomaterials* **1987**, *8*, 142−145.

(17) Rawls, H. R.; Starr, J.; Kasten, F. H.; Murray, M.; Smid, J.; Cabasso, I. Radiopaque acrylic resins containing miscible heavy-metal compounds. *Dent. Mater.* **1990**, *6*, 250−255.

(18) Davy, K. W. M.; Anseau, M. R.; Odlyha, M.; Foster, G. M. X-ray Opaque Methacrylate Polymers for Biomedical Applications. *Polym. Int.* **1997**, *43*, 143−154.

(19) Emans, P. J.; Saralidze, K.; Knetsch, M. L. W.; Gijbels, M. J. J.; Kuijer, R.; Koole, L. H. Development of new injectable bulking agents: Biocompatibility of radiopaque polymeric microspheres studied in a mouse model. *J. Biomed. Mater. Res., Part A* **2005**, *73*, 430−436.

(20) Horák, D.; Metalová, M.; Rypáček, F. New radiopaque polyHEMA-based hydrogel particles. *J. Biomed. Mater. Res.* **1997**, *34*, 183−188.

DOI: 10.1021/acsomega.6b00373
ACS Omega 2017, 2, 755−764

(21) Moszner, N.; Salz, U.; Klester, A. M.; Rheinberger, V. Synthesis and polymerization of hydrophobic iodine-containing methacrylates. *Angew. Makromol. Chem.* **1995**, *224*, 115−123.
(22) Francis, N. K.; Pawar, H. S.; Ghosh, P.; Dhara, S. In Situ Iodination Cross-Linking of Silk for Radio-Opaque Antimicrobial Surgical Sutures. *ACS Biomater. Sci. Eng.* **2016**, *2*, 188−196.
(23) Leggat, P. A.; Kedjarune, U. Toxicity of methyl methacrylate in dentistry. *Int. Dent. J.* **2003**, *53*, 126−131.
(24) Leggat, P. A.; Smith, D. R.; Kedjarune, U. Surgical applications of methyl methacrylate: A review of toxicity. *Arch. Environ. Occup. Health* **2009**, *64*, 207−212.
(25) Moreau, M. F.; Chappard, D.; Lesourd, M.; Monthéard, J. P.; Baslé, M. F. Free radicals and side products released during methylmethacrylate polymerization are cytotoxic for osteoblastic cells. *J. Biomed. Mater. Res.* **1998**, *40*, 124−131.
(26) Sabokbar, A.; Fujikawa, Y.; Murray, D. W.; Athanasou, N. A. Radio-opaque agents in bone cement increase bone resorption. *J. Bone Jt. Surg., Br. Vol.* **1997**, *79*, 129−134.
(27) Whysner, J. Benzene-induced genotoxicity. *J. Toxicol. Environ. Health, Part A* **2000**, *61*, 347−351.
(28) Whysner, J.; Reddy, M. V.; Ross, P. M.; Mohan, M.; Lax, E. A. Genotoxicity of benzene and its metabolites. *Mutat. Res., Rev. Mutat. Res.* **2004**, *566*, 99−130.
(29) Yardley-Jones, A.; Anderson, D.; Jenkinson, P. C.; Lovell, D. P.; Blowers, S. D.; Davies, M. J. Genotoxic effects in peripheral blood and urine of workers exposed to low level benzene. *Br. J. Ind. Med.* **1988**, *45*, 694−700.
(30) Johnson, S. B.; Dunstan, D. E.; Franks, G. V. A novel thermally-activated crosslinking agent for chitosan in aqueous solution: A rheological investigation. *Colloid Polym. Sci.* **2004**, *282*, 602−612.
(31) Friedman, M. Applications of the Ninhydrin Reaction for Analysis of Amino Acids, Peptides, and Proteins to Agricultural and Biomedical Sciences. *J. Agric. Food Chem.* **2004**, *52*, 385−406.
(32) Johnson, S. B.; Dunstan, D. E.; Franks, G. V. A novel thermally-activated crosslinking agent for chitosan in aqueous solution: A rheological investigation. *Colloid Polym. Sci.* **2004**, *282*, 602−612.
(33) *United States Pharmacopeia and National Formulary (USP 29-NF 24)*; United States Pharmacopeia Convention: Rockville, MD, 2010; Vol. 2.
(34) Ungureanu, C.; Ioniţă, D.; Berteanu, E.; Tcacenco, L.; Zuav, A.; Demetrescu, I. Improving Natural Biopolymeric Membranes Based on Chitosan and Collagen for Biomedical Applications Introducing Silver. *J. Braz. Chem. Soc.* **2015**, *26*, 458−465.
(35) Selvakumar, M.; Pawar, H. S.; Francis, N. K.; Das, B.; Dhara, S.; Chattopadhyay, S. Excavating the Role of Aloe Vera Wrapped Mesoporous Hydroxyapatite Frame Ornamentation in Newly Architectured Polyurethane Scaffolds for Osteogenesis and Guided Bone Regeneration with Microbial Protection. *ACS Appl. Mater. Interfaces* **2016**, *8*, 5941−5960.
(36) Breen, A.; Mc Redmond, G.; Dockery, P.; O'Brien, T.; Pandit, A. Assessment of Wound Healing in the Alloxan-Induced Diabetic Rabbit Ear Model. *J. Investig. Surg.* **2008**, *21*, 261−269.
(37) Selvakumar, M.; Srivastava, P.; Pawar, H. S.; Francis, N. K.; Das, B.; Sathishkumar, G.; Subramanian, B.; Jaganathan, S. K.; George, G.; Anandhan, S.; Dhara, S.; Nando, G. B.; Chattopadhyay, S. On-Demand Guided Bone Regeneration with Microbial Protection of Ornamented SPU Scaffold with Bismuth-Doped Single Crystalline Hydroxyapatite: Augmentation and Cartilage Formation. *ACS Appl. Mater. Interfaces* **2016**, *8*, 4086−4100.
(38) Romani, A. A.; Ippolito, L.; Riccardi, F.; Pipitone, S.; Morganti, M.; Baroni, M. C.; Borghetti, A. F.; Bettini, R. In Vitro Blood Compatibility of Novel Hydrophilic Chitosan Films for Vessel Regeneration and Repair **2013**.10.5772/52706
(39) Friedman, M. Applications of the ninhydrin reaction for analysis of amino acids, peptides, and proteins to agricultural and biomedical sciences. *J. Agric. Food Chem.* **2004**, *52*, 385−406.
(40) Roberts, I.; Kimball, G. E. The Halogenation of Ethylenes. *J. Am. Chem. Soc.* **1937**, *59*, 947−948.
(41) Moulay, S. Molecular iodine/polymer complexes. *J. Polym. Eng.* **2013**, *33*, 389.
(42) Pawar, H. S.; Francis, N. K.; Rameshbabu, A. P.; Dhara, S. 2,5-Dihydro-2,5-dimethoxyfuran crosslinked silk-chitosan blend tubular construct for vascular graft application. *Mater. Today Commun.* **2016**, *8*, 139−147.
(43) Mackenzie, D. The history of sutures. *Med. Hist.* **1973**, *17*, 158−168.
(44) Lober, C. W.; Fenske, N. A. Suture materials for closing the skin and subcutaneous tissues. *Aesthetic Plast. Surg.* **1986**, *10*, 245−247.
(45) Bigi, A.; Cojazzi, G.; Panzavolta, S.; Rubini, K.; Roveri, N. Mechanical and thermal properties of gelatin films at different degrees of glutaraldehyde crosslinking. *Biomaterials* **2001**, *22*, 763−768.
(46) Yang, D.-J.; Jeon, J.-H.; Lee, S.-Y.; An, H.-W.; Park, K. O.; Park, K.-B.; Kim, S. Effects of Collagen Grafting on Cell Behaviors in BCP Scaffold with Interconnected Pore Structure. *Biomater. Res.* **2016**, *20*, 1−7.
(47) Michel, J.; Genet, C. C. D.-G.; Rouxhet, P. G. *Medical Applications of Colloids*; Springer-Verlag: New York, 2008.
(48) Hai-Fang, W.; Xiao-Yong, D.; Jing, W.; Xing-Fa, G.; Geng-Mei, X.; Zu-Jin, S.; Zhen-Nan, G.; Yuan-Fang, L.; Yu-Liang, Z. XPS Study of C£-I Covalent Bond on Single-walled Carbon Nanotubes (SWNTs)[a3]. *Acta Phys. Chim. Sin.* **2004**, *20*, 673−675.
(49) Sundararaghavan, H. G.; Monteiro, G. A.; Lapin, N. A.; Chabal, Y. J.; Miksan, J. R.; Shreiber, D. I. Genipin-induced changes in collagen gels: Correlation of mechanical properties to fluorescence. *J. Biomed. Mater. Res., Part A* **2008**, *87*, 308−320.
(50) Ghosh, P.; Rameshbabu, A. P.; Das, D.; Francis, N. K.; Pawar, H. S.; Subramanian, B.; Pal, S.; Dhara, S. Covalent cross-links in polyampholytic chitosan fibers enhances bone regeneration in a rabbit model. *Colloids Surf., B* **2015**, *125*, 160−169.
(51) Joseph, B. L.; Shurvell, H. F.; Cooks, R. G. *Introduction to Organic Spectroscopy*, 1st ed.; Macmillan: New York, 1987; Vol. *1*, pp 174−177.
(52) Zhou, L. H.; Nahm, W. K.; Badiavas, E.; Yufit, T.; Falanga, V. Slow release iodine preparation and wound healing: In vitro effects consistent with lack of in vivo toxicity in human chronic wounds. *Br. J. Dermatol.* **2002**, *146*, 365−374.
(53) Thorn, R. M. S.; Austin, A. J.; Greenman, J.; Wilkins, J. P. G.; Davis, P. J. In vitro comparison of antimicrobial activity of iodine and silver dressings against biofilms. *J. Wound Care* **2009**, *18*, 343−346.
(54) van Meerloo, J.; Kaspers, G. J. L.; Cloos, J. Cell sensitivity assays: The MTT assay. *Methods in Molecular Biology*, 2011; Vol. *731*, pp 237−245.
(55) Okada, T.; Hayashi, T.; Ikada, Y. Degradation of collagen suture in vitro and in vivo. *Biomaterials* **1992**, *13*, 448−454.
(56) Chu, C. C. *Polymeric Biomaterials, Revised and Expanded*, 2nd ed.; CRC Press, 2001.
(57) Shi, L.; Ermis, R.; Garcia, A.; Telgenhoff, D.; Aust, D. Degradation of human collagen isoforms by Clostridium collagenase and the effects of degradation products on cell migration. *Int. Wound J.* **2010**, *7*, 87−95.
(58) Labaf, A.; Själander, A.; Stagmo, M.; Svensson, P. J. INR variability and outcomes in patients with mechanical heart valve prosthesis. *Thromb. Res.* **2015**, *136*, 1211−1215.
(59) Peters, R. H.; van den Besselaar, A. M.; Olthuis, F. M. Determination of the mean normal prothrombin time for assessment of international normalized ratios. Usefulness of lyophilized plasma. *Thromb. Haemostasis* **1991**, *66*, 442−445.
(60) Kottke-Marchant, K.; Anderson, J. M.; Umemura, Y.; Marchant, R. E. Effect of albumin coating on the in vitro blood compatibility of Dacron arterial prostheses. *Biomaterials* **1989**, *10*, 147−155.

DOI: 10.1021/acsomega.6b00373
ACS Omega 2017, 2, 755−764